Influence of the Main Process Parameters on the Physical and Mechanical Properties of the Bottom Ash Ceramics

Biljana Angjusheva[1], Emilija Fidancevska[1], Vilma Ducman[2]

[1]Faculty of Technology and Metallurgy, Ss Cyril and Methodius University in Skopje, Skopje, Republic of Macedonia
biljana@tmf.ukim.edu.mk

[2]Slovenian National Building and Civil Engineering Institute, Ljubljana, Slovenia, biljana@tmf.ukim.edu.mk

Abstract: Bottom ash has been presented as a major problem of disposal throughout the world, since it is produced from the process of coal combustion in thermal power plants. However, its physical and chemical properties make the bottom ash an adequate potential construction material in variety of applications.

The aim of the study was to investigate the possibility of utilization of bottom ash for production of ceramics compacts and to analyse the influence of the main process parameters and their interaction on the physical and mechanical properties of the final product.

Consolidation of the powders was conducted on two bottom ash samples with particle size (S) -0.250+0.125 mm and -0.500+0.250 mm, pressing pressure (P) of 100 and 150 MPa and sintering temperature (T) of 1100 and 1150 ℃. The density (ρ) and bending strength (σ) of the dense bottom ash compacts were the response function. The optimization was performed through implementation of main effect plots, Pareto charts and 3D surface method using "Statgraphics Centurion" software package.

The obtained model equations of the density and bending strength dependence from the main process parameters are solid basic data for modeling the process of ceramic production.

Keywords: bottom ash, optimization, ceramics, bending strength, density.

Introduction

Coal-fired power stations produce large quantities of solid waste causing economical and environmental problems. During coal combustion its organic components are incinerated, but its inorganic components remain mostly in the plant's by-products. These residues i.e. the by-products are known as ash, hence two types of ash are differentiated: fly ash (FA) and bottom ash (BA).

The coal is a dominant resource for production of electricity in Macedonia, where more than 72% of the electrical power requirements are generated by REK Bitola, a large lignite power plant located nearby Bitola (ELEM, Macedonian Power Plants, www.elem.com.mk). A certain quantity of the produced fly ash from the power plant is used by local cement plant TITAN Cementarnica "Usje" while the rest of the fly ash and all amount of bottom ash are deposited at local dumps.

The physical and chemical properties of coal bottom ash are influenced by the coal source, type of coal burner and the operating conditions of the burner (Duminda and Van Hullebusch , 2014). Therefore this determines the chemical composition of coal bottom ash which is consisted of silicates, carbonates, aluminate, ferrous materials and metalloids. As to its physical appearance, bottom ash is an angular material of porous surface texture and ranges from fine gravel to coarse gravel in contrast to the fine structure of fly ash (Kantiranis, Georgakopoulos, Filipidis and Drakoulis, 2004; Kim and Lee, 2011). Compared to fly ash bottom ash utilization rate is smaller than the fly ash (European Coal Combustion Products Association, www.ecoba.com).

There are several papers dealing with high volume utilization of bottom ash. Presented data (Kim, Prezzi and Salgado, 2005) for geotechnical properties of bottom and fly ash mixtures for use in highway

embankments pointing that if the environmental requirements are satisfied the ash mixtures can provide fill material with comparable strength and compressibility to most soils typically used as fillers. Bajare, Bumanis and Upeniece (2013) reported the usage of bottom ash as microfiller for traditional concrete, concluding that is possible to decrease the price of concrete C30/37 by 10% and reduce the amount of CO_2 emission by 22.9% by usage of grinded coal bottom ash. Authors Tocçu, Toprak and Uygunoğlu (2014) and Kim and Do (2012) reveal the possibility for alkali activation of coal bottom ash and synthesis and development of composite geomaterial and geopolymers cement. In the paper (Arenas, Marrero, Levia, Guzman and Arenas, 2011) authors described the method of production of high fire resistance blocks containing different composition of Portland cement type II, sand and coal combustion fly ashes. The results show that the replacement of fine aggregate with fly ash and coarse aggregate with bottom ash have a remarkable influence on fire resistance and cause no detriment to the mechanical properties of the product.

Another possible application of bottom ash is as raw material for ceramic (Benavidez, Grasselli and Quaranta, 2003) and glass-ceramics (Choi and Kang, 2009). Tayler and Daidone (2011) examined the characteristics of bottom ash as well as the beneficial effects that bottom ash provides to a brick making raw material and brick making process. They concluded that use of bottom ash in the clay body has been very effective in reducing stabilizing the drying and firing shrinkage.

Response surface method is powerful tool for optimazing experimental condition for maximasing or minimasing various responces (NIST/SEMATECH e-Handbook of Statistical Methods, 2012). By designing and analizing of experiments we can optimized the efective parameters with a minimum number of experiments.

The main objective of this study is to investigate the possibility for production of ceramic using bottom ash as raw material and to evaluate efficiency of the sintering process influenced by multiple parameters such as sintering temperature, particle size and pressing pressure.

MATERIALS AND METHODS

The bottom ash (BA, as-received) collected from the thermal power plant "REK Bitola" from Republic of Macedonia was dried at 100-110^{0}C to constant weight then sieved through set of sieves +1mm–63µm. Samples of bottom ash with particle size -500+250 µm (coded BA1) and -250+125 µm (coded BA2) were subject of this investigation.

Determination of the morphological characteristic of the bottom ash was carried out by scanning electron microscopy (SEM) in a JEOL JSM 5500LV. The powders were coated with gold prior to examination. The coating was performed at apparatus model BAL-TEC/SCD005 with gold at current 35mA for 120s.

Chemical composition was determined with XR Fluorescence, model ARL 9900XP. Loss of ignition (LOI) in the ash was determined from the mass loss after 2 hours at temperature of 800^{0}C. The powders BA1 and BA2 were heated at 800^{0}C/2h before consolidation.

Specific gravity of the examined bottom ash was determined by pycnometric method.

Consolidation of the powders was perform using distilled water as binder than uniaxial cold pressed (Weber Pressen KIP 100) at 100MPa and 150MPa obtaining compacts with average dimensions of 60mm x 5mm x 5mm. Sintering of the compacted samples were done at 1100^{0}C and 1150^{0}C with a heating rate of 5^{0}C/min and isothermal treatment at the final temperature of 60 min, under normal atmospheric conditions. The bulk density of the sintered samples was determined by the water displacement method according to EN-993.

The bending strength of the investigated samples was determined by means of a 3-point bending strength tester (Netzsch 401/3), with a span of 30mm and a 0.5mm/min loading rate.

The optimization was achieved when the influence of the three parameters: sintering temperature, applied pressure and particle size was analyzed on the predicted responses namely bending strength and density of the ceramics. Created factorial design studied the effects of 3 factors in 8 runs. The design runs in the single block. To provide the protection against the effect of lurking variables the experiment has been fully randomized. For that purpose the software package *Statgraphics Centurion* was used and from its options we were able to obtain 3D surface model, Pareto chart and main effects plot for both investigated responses and the results are presented in graphical and analytical form.

Results and discussion

The chemical composition of BA samples, Table 1, showed that the main components are: SiO_2, Al_2O_3, Fe_2O_3 and CaO. The as-received bottom ash contains a greater amount of coal determined by LOI (48.7 wt%), while for BA1 and BA2, the LOI values are 11.85 and 13.18 wt%, respectively. High level of residual carbon may lead to difficulties in carbon burnout in the firing process resulting on black coring and even bloating (Tayler and Daidone, 2011).

Table 1. Chemical composition of the BA samples

Sample	Oxide (wt%)								
	SiO_2	Al_2O_3	Fe_2O_3	CaO	K_2O	Na_2O	SO_3	TiO_2	LOI
BA, as-received	33.46	9.11	2.81	2.38	1.33	0.51	0.47	0.29	48.7
BA1	57.80	15.73	4.85	4.11	2.29	0.88	0.81	0.50	11.85
BA2	57.02	15.52	4.78	4.05	2.26	0.86	0.80	0.48	13.18

Fig. 1 shows morphology of BA1 and BA2 powders. Beside dimensions of the particles which is the major difference between the samples BA1 and BA2 both powders have similar morphology. Particles with irregular geometry are observed in the both SEM micrographs. Dark porous particles belong to the coal particles present in the ash, while shiny angular particles are mineral particles from the different phases present in the ash. Some small spherical particles can be observed brought principally by fly ash.
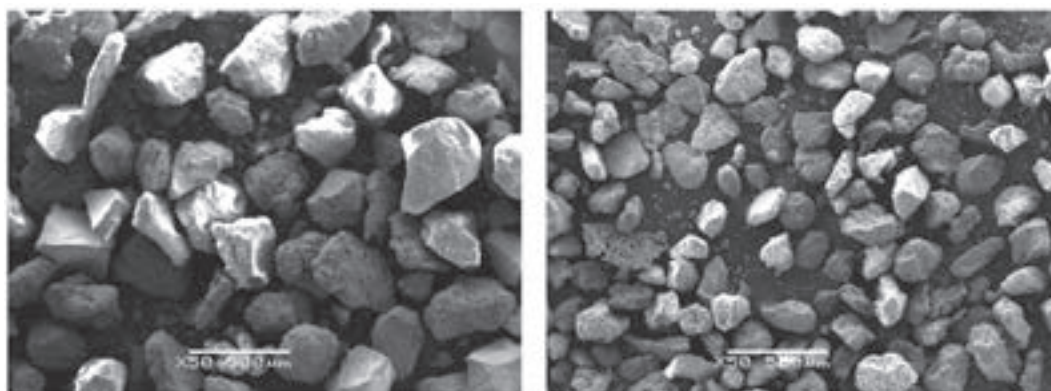
BA1, bar 500mm, x50   BA2, bar 500mm, x50

Figure 1. SEM Micrographs of the BA1 and BA2

The obtained data for specific gravity of 2.50 and 2.62 g/cm^3 for BA1 and BA2 are in accordance with data reported in literature (Kim and Lee, 2015).

In order to produce the dense ceramic compacts two samples of bottom ash particles BA1 and BA2 was consolidated by previously described procedure. Optimization process was based on the influence of

three main process parameters: sintering temperature, particle size and applied pressure. For that aim was obtained the following graphical data that allows us to state the influence of the parameters on the density and bending strength. Samples sintered at temperature lower than 1100ºC shows very weak mechanical properties for both samples of BA, so the optimization process was conducted with temperature higher than 1100 ºC. By analyzing the Pareto chart (Fig. 2) it is evident that the density of the BA samples is directly dependent of the sintering temperature and the particle size, for which favorable are high temperature points and narrower particle size (Fig. 3).
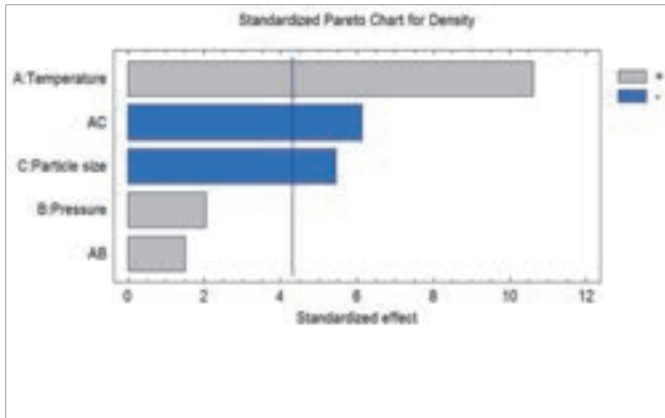
Figure 2. Pareto chart of the main process parameters and their interactions on the density of BA ceramics
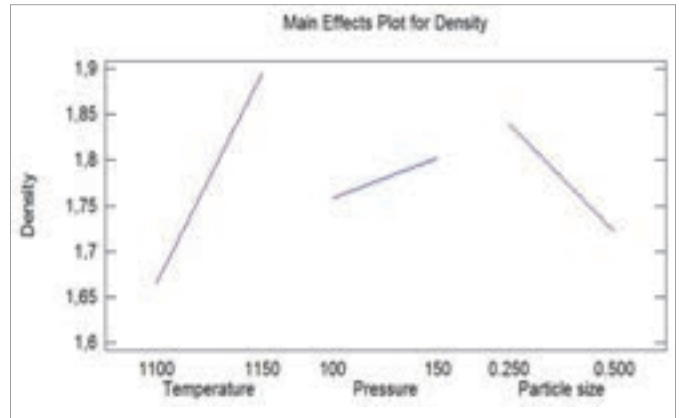

Figure 3. Statistic influences of the main process parameters and their interactions on the density of BA ceramics
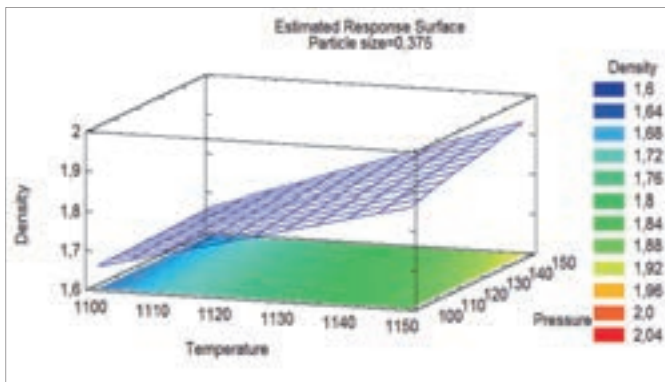

Figure 4. 3D optimization diagram of the main effects at variable temperature (°C), pressure (MPa) and constant particle size (mm)
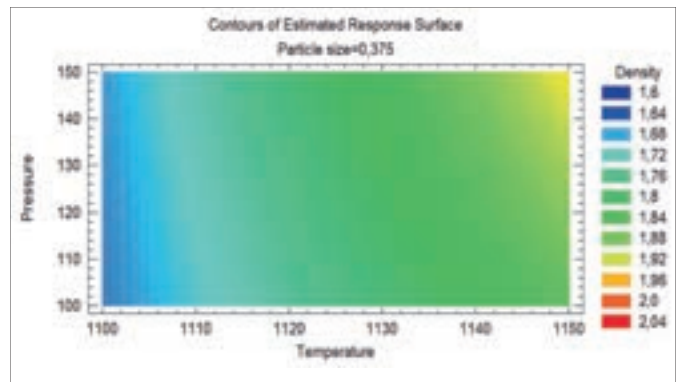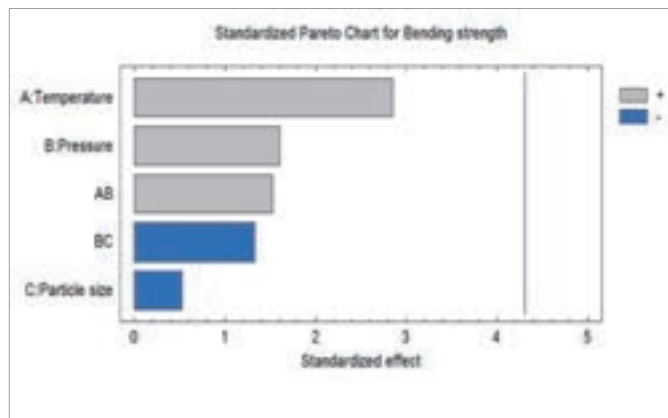

Figure 5. Optimization diagram of the main effects at variable temperature (°C), pressure (MPa) and constant particle size (mm)

In the line with the obtained data from the software package, according to the influences of the main parameters the final model equation for density is presented as:

$$Density = -8.7055 + 0.00938 * T - 0.02836 * P + 23.556 * S - 0.000026 * T * P - 0.02136 * T * S \quad (1)$$

where T is the temperature (ºC); P is the pressing pressure (MPa); S is particle size (mm). The above equation suggested by the software is based on the linear model for density as response function. In addition, the 3D optimization diagram (Fig. 4) display the optimal maximum for the density (1.9-2 g/cm³) which has begun appearing in the range of 1130ºC and 1150°C and pressure 150 MPa. The maximum begins approximately from the middle of the graphic and moving to the upper right corner, as it can be noted from Fig. 5.
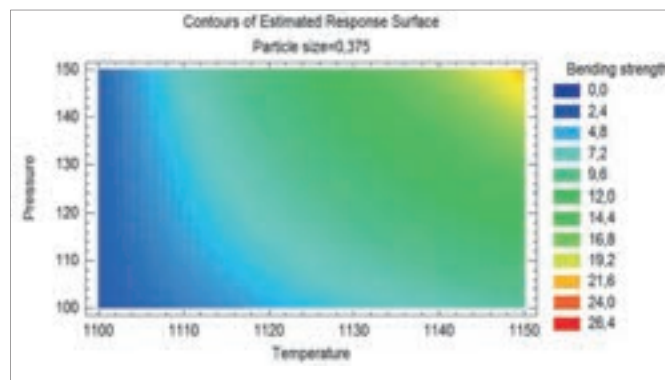
Figure 6. Pareto chart of the main process parameters and their interactions on the bending strength of BA ceramics
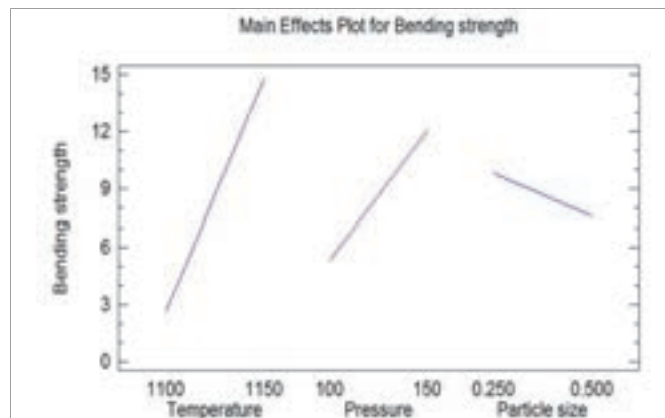
Figure 7. Statistic influence of the main process parameters and their interactions on the bending strength of BA samples
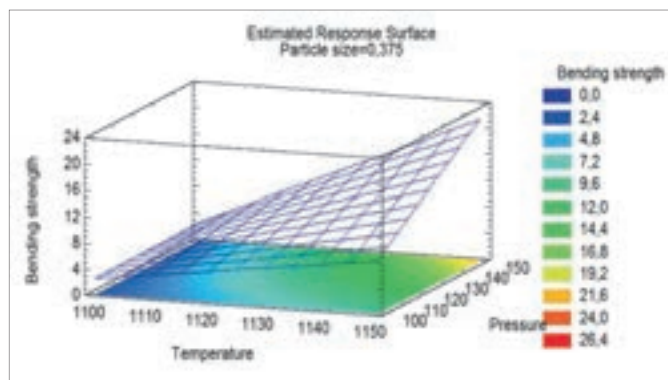
Figure 8. 3D optimization diagram of the main effects at variable temperature (°C), pressure (MPa) and constant particle size (mm)

Figure 9. Optimization diagram of the main effects at variable temperature (°C), pressure (MPa) and constant particle size (mm)

In the case of optimizing the bending strength of BA, the response was inspected as a function of the process parameters. By analyzing the Pareto chart (Fig. 6), evidently the bending strength of the BA samples is directly dependent of higher sintering temperature until reaching one optimal point. On the other hand, the influence of the particle size on the mechanical properties is lower compared with the other parameters (Fig. 7), but more desirable particle distribution is the lower one, as the Pareto chart indicates.

In line with the results the process of optimization presented by "Statgraphics Centurion", the final model equation of the bending strength dependence is:

$$\text{Bending strength} = 260.268 - 0.2735 * T - 5.3833 * P + 507.38 * S + \\ + 0.005208 * T * P - 0.3584 * T * S - 0.9048 * P * S \quad (2)$$

From the 3D optimization diagram (Fig. 8) it is evident that optimal maximum for the bending strength (20-24 MPa) was obtained at sintering temperature 1150°C and pressure (140-150 MPa) presented in the diagrams with the green zone, which begins approximately from the second third of the graph and moves to the upper right corner (Fig. 9).

The microstructure of the obtained ceramics from BA1 sintered at 1150ºC, P=100 MPa and P= 150MPa are presented in the Figsures 10 and 11. Microstructure of the fractured sample BA1, sintered at 1150ºC, P= 150 MPa (Fig. 11) shows little bit more uniform surface as compared to BA1 sintered at 1150ºC, P= 100 MPa (Fig.10) because the sample has higher packaging density due to the applied higher pressing pressure during the consolidation. Open irregular connected pores are more present in the speci-

men presented in Fig. 10 also due to the lower packaging density. Spherical closed micro pores can be observed in both microstructures obtained from the porous particles present in the ash. It is evident the regions which showed liquid-phase sintering (Figs. 10 and 11). Small cracks are also visible in both microstructures which could be due to the shrinkage of the samples during the cooling.
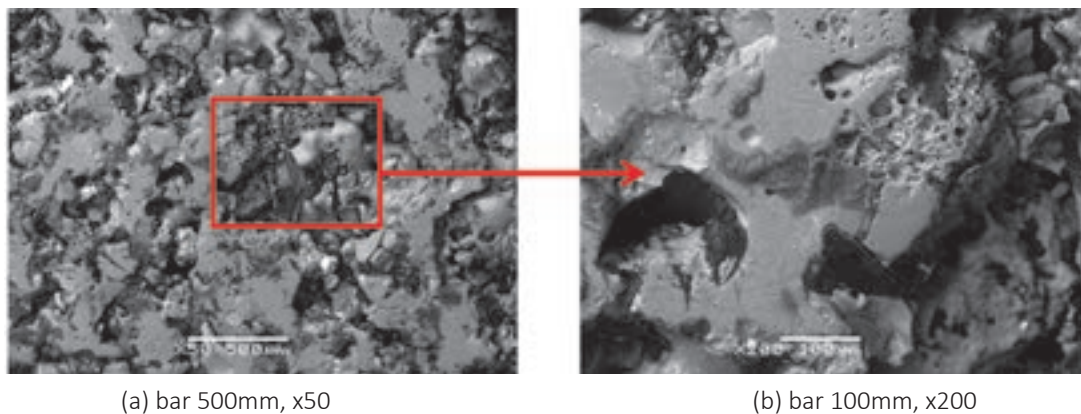
(a) bar 500mm, x50   (b) bar 100mm, x200
Figure 10. Microstructure of the fractured ceramics from BA1, sintered at 1150°C, P=100MPa
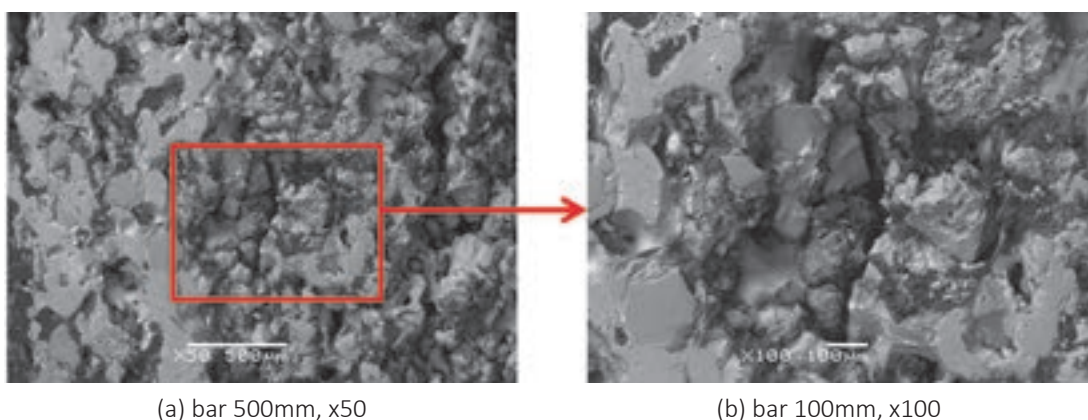
(a) bar 500mm, x50   (b) bar 100mm, x100
Figure 11. Microstructure of the fractured ceramics from BA1, sintered at 1150 °C, P=150 MPa

Conclusion

This study investigated the possibility to product dense ceramics using coal bottom ash produced from the power plant REK Bitola, R. Macedonia. By using the 3D optimization method the efficiancy of the sintering process was evaluated by multiple parameters such as sintering temperature, particle size and pressing pressure.

It was concluded that the major role in achieving better mechanical properties would be accomplished with higher temperature points and the optimal applied pressure. Furthermore, the highest densities of sintered compacts are directly related with narrower particle size distribution.

The final model equations for density and bending strength dependence from the main process parameters are:

$$\text{Density} = -8.7055 + 0.00938 * T - 0.02836 * P + 23.556 * S - 0.000026 * T * P - 0.02136 * T * S$$

$$\text{Bending strength} = 260.268 - 0.2735 * T - 5.3833 * P + 507.38 * S +$$
$$+ 0.005208 * T * P - 0.3584 * T * S - 0.9048 * P * S$$

Yet, there needs to be done further investigation in order to collect more data regarding other process parameters influencing the physical and mechanical properties of the bottom ash to produce dense ceramics which would be reused properly.

References

Arenas, C. G., Marrero, M., Levia, C., Guzmán, J.S. & Arenas, L.F.V. (2011). High fire resistance in blocks containing coal combustion fly ashes and bottom ash. Waste Management, 31, 1711-1789.

Bajare, D., Bumanis, G. & Upeniece, L. (2013). Coal combustion bottom ash as microfiller with pozzolanic properties for traditional concrete. Procedia Engineering, 57, 149-158.

Benavidez, E., Grasseli, C. & Quaranta, N. (2003). Densification of ashes from a thermal power plant. Ceramics International, 29, 61-68.

Duminda, J. & Van Hullebusch, E.D. (2014). Reuse options for coal fired power plant bottom ash and fly ash. Reviews in Environmental Science and Biotechnology, 13(4), 467-486.

European Coal Combustion Products Association, www.ecoba.com, Accessed 28.04.2015

ELEM, Macedonian Power Plants http://www.elem.com.mk/ Accessed 28.04.2015

Kantiranis, N., Georgakopoulos, K., Filipidis, A. & Drakoulis, A. (2004). Mineralogy and organic matter content of bottom ash samples from Agios Dimitrios plant, Greece. In Proceedings of the 10th International Congress, Thessaloniki, April , 320-321.

Kim, B., Prezzi, M. & Salgado, R. (2005). Geotechnical properties of fly and bottom ash mixture for use in highway embankments. Journal of Geotechnical and Geoenvironmental Engineering, 131(7), 914-924.

Kim, H.K. & Lee, H.K. (2015). Coal Bottom Ash in Field of Civil Engineering: A Review of Advanced Application and Environmental Consideration. Journal of Civil Engineering, 19(6), 1802-1818.

Kim, H.K. & Lee, H.K. (2011). Use of power plant bottom ash as fine and coarse aggregates in high-strength concrete. Construction and Building Materials, 25, 1115-1122.

Kim, Y. & Do, T.H. (2012). Effect of bottom ash particle size on strength development in composite geomaterial. Engineering Geology, 139-140, 85-91.

Naganathan, S., Subramaniam, N. & Nasharuddin, B.M.K. (2012). Development of brick using thermal power plant bottom ash and fly ash. Asian Journal of Civil Engineering, 13 (1), 275-287.

NIST/SEMATECH e-Handbook of Statistical methods (2012), http://www.itl.gov/div898/handbook/, Accessed 28.04.2015

Tayler, V. G. & Daidone, W. (2011). The use of bottom ash in the manufacture of clay face brick, 11 WOCA Conference, 9-12 May, Denver USA.

Tocçu, I.B., Toprak, M. U. & Uygunoğlu, T. (2014). Durability and microstructure characteristics of alkali activated coal bottom ash geopolymer cement. Journal of Cleaner Production, 81, 211-217.